Annales Geophysicae

Ionospheric $f o$F2 anomalies during some intense geomagnetic storms

R. P. Kane

Instituto Nacional de Pesquisas Espacias, São Jose dos Campos, São Paulo, Brazil

Abstract. The global evolutions of $f o$F2 anomalies were examined for three very intense geomagnetic storms, namely the Halloween events of October–November 2003 (Event X, 29–30 October 2003, D_{st} −401 nT; Event Y, 20–21 November 2003, D_{st} −472 nT), and the largest D_{st} storm (Event Z, 13–14 March 1989, D_{st} −589 nT). For Event X, troughs (negative storms) were clearly seen for high northern and southern latitudes. For northern midlatitudes as well as for low latitudes, there were very strong positive effects on 29 October 2003, followed by negative effects the next day. For Event Y, there were no troughs in NH high latitudes for morning and evening hours but there were troughs for night. For midlatitudes and low latitudes, some longitudes showed strong negative effects in the early morning as expected, but some longitudes showed strong positive effects at noon and in the evening hours. Thus, there were many deviations from the model patterns. The deviations were erratic, indicating considerable local effects superposed on general patterns. A disconcerting feature was the presence of strong positive effects during the 24 h before the storm commencement. Such a feature appears only in the 24 h before the geomagnetic storm commencement but not earlier. If genuine, these could imply a prediction potential with a 24-h antecedence. For Event Z (13–14 March 1989, equinox), all stations (all latitudes and longitudes) showed a very strong "negative storm" in the main phase, and no positive storms anywhere.

Keywords. Ionosphere (Equatorial ionosphere – Ionospheric disturbances – Mid-latitude Ionosphere – Polar ionosphere)

1 Introduction

The ionospheric F2 region has average patterns of daily and seasonal variations. These patterns have considerable day-to-day variations, but spectacular changes occur (positive or negative anomalies) during geomagnetic storms, when there

Correspondence to: R. P. Kane
(Kane@dge.inpe.br)

is an input of energy (from solar wind) into the polar ionosphere (Danilov, 2001). Thermospheric composition, temperature and circulation changes occur, which affect the electron concentration in the F2 region and the heated gas spreads from polar to lower latitudes. A conflict between the storm-induced circulation and the regular one determines the spatial distribution of negative and positive phases in different seasons. The relative importance of horizontal winds and down-welling in causing long-duration positive storm effects has not been determined yet (Buonsanto, 1999), but specifically, the expected patterns are roughly as follows:

1. High latitudes: Deep troughs of ionization at night at high and subauroral latitudes, often accompanied by enhancements in electron temperature, electric fields and ion outflow. During storms, extended troughs at progressively lower latitudes during the course of the night. Narrow troughs are associated with localized electric field enhancements, while extended troughs can span several degrees of latitude equatorward of the region of diffuse aurora, associated with flux tubes which "stagnate" and convect westward for extended periods through the nightside, allowing the plasma to steadily recombine.

2. Dusk effect: After a geomagnetic storm SSC, large enhancements in NmF2 and TEC in the afternoon and evening hours, earlier at higher latitudes.

3. Long duration positive storm effects: Caused by downwelling of neutral atomic oxygen and uplifting of the F layer due to winds. Both of these rely on large-scale changes in the thermospheric circulation caused by heating in the auroral zone.

4. Negative phase: The ionospheric storm negative phase in NmF2 and TEC occurs in a composition disturbance zone which reaches lower latitudes in summer than in winter and has a preference for the night and morning sectors due to the local time variation of the neutral winds.
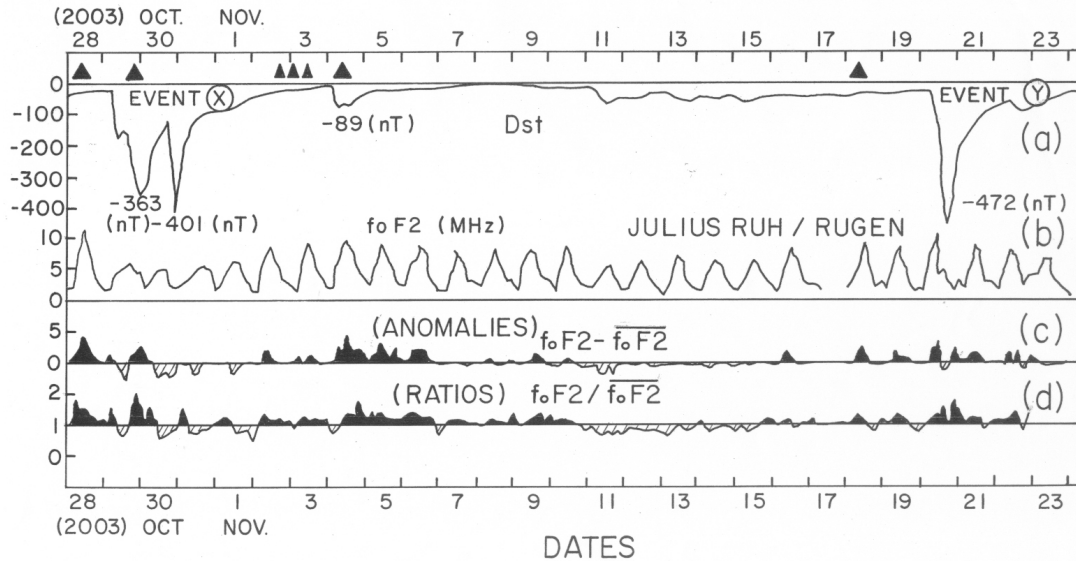
Fig. 1. Plots for the 27-d interval 28 October–23 November 2003 of the hourly values of **(a)** geomagnetic D_{st}, **(b)** ionospheric $f o$F2 at the midlatitude European location Juliusruh/Rügen (54.6° N, 13.4° E), **(c)** $f o$F2 anomalies, **(d)** $f o$F2 ratios. Positive deviations and ratios above 1.0 are painted black, negative deviations and ratios below 1.0 are shown as hatched. The triangles indicate solar flare occurrences.

5. Low latitude and equatorial zone: The $\boldsymbol{E} \times \boldsymbol{B}$ drifts are affected by prompt penetration of magnetospheric convection electric fields, as well as by longer-lived dynamo electric fields from the disturbance neutral winds and storm-related changes in ionospheric conductivity (Fejer, 1997). In addition to the drifts caused by electric fields, TADs and also longer duration disturbances in the global thermospheric circulation with resulting neutral composition changes have important effects on the low latitude region during storms.

6. Even under geomagnetically quiet conditions, electron density is extremely variable in the equatorial zone between sunset and midnight due to the presence of irregularities with scale sizes ranging from less than 1 m to greater than 200 km. How geomagnetic storms affect the development of equatorial irregularities depends on longitude but varies considerably from storm-to-storm.

Ionospheric storms associated with geomagnetic storms have been studied copiously in the past, for individual locations, for groups of locations, and on a global basis, for one or many storms (Prölss, 1997, and references therein; Szuszczewicz et al., 1998, and references therein). Since IGY, the largest geomagnetic storm occurred on 13 March 1989 (D_{st} −589 nT). However, two very intense storms occurred recently in quick succession, namely Halloween events of 29–31 October 2003 (D_{st} −401 nT), and 20 November 2003 (D_{st} −472 nT). In the present communication, the morphology of ionospheric $f o$F2 anomalies is illustrated for these storms.

2   Data

All data were obtained from the NGDC SPIDR website http://spidr2.ngdc.noaa.gov/spidr/. Data quality and continuity were not always good. The $f o$F2 values could have errors due the presence of spread F and many other factors. In the SPIDR data, values of $f o$F2 are given as simple numbers, with no qualified coding. Hence, effects due to spread F, etc., cannot be ruled out and could be important, particularly for low latitudes. However, scrutiny of these would need access to original, detailed data from individual locations, which is a laborious process. These cannot be considered in detail in a general analysis like the present one, and no scrutiny of data of any kind was done. We expect (hopefully) that errors would be minimized in averages. With $f o$F2, data for hmF2 would be of great importance, but these were mostly meagre or absent and hence, are not considered here.

3   The Halloween events of October–November, 2003 (Events X and Y)

Figure 1a shows a plot of hourly D_{st} values during the 27-day interval 28 October–23 November 2003. The first storm (henceforth called Event X) started at ∼06:00 UT on 29 October, reached a maximum depression of −363 nT at 00:00 UT of 30 October (main phase of 18:00 h), recouped but had a second maximum depression of −401 nT at 22:00 UT on 30 October, and then recovered, first rapidly and then slowly. Thus, this was a complex storm. The triangles indicate solar flare occurrences. There were two strong solar flares, one on 28 October and another on 29 October. The second storm (henceforth called Event Y) started at ∼11:00 UT of 20 November, reached a maximum depression

of -472 nT at 19:00 UT of 20 November (main phase of 9 h), and then recovered first rapidly, then slowly. There was a strong solar flare on 18 November. In between, there was a small storm on 4 November (D_{st} -89 nT). There was a very, very intense solar flare on 4 November (largest in known history, so far), but it was a limb flare, without emissions (CMEs) directed towards the Earth and no terrestrial disturbances were produced. The mild storm of 4 November was caused by less strong solar flares, which occurred on 2–3 November.

Figure 1b shows a plot of hourly $f o$F2 (MHz) at the location Juliusruh/Rügen (54.6° N, 13.4° E) in European mid-latitude, LT about 1 h ahead of UT. There is a substantial daily variation, with a maximum of $\sim$7–10 MHz at about noon and a minimum of $\sim$1–2 MHz soon after midnight. The storm effects are superposed on this background daily variation. To isolate the storm effects, the background daily variation needs to be subtracted. In conventional methods, the background is estimated as a monthly mean. However, this may become polluted by storm days. In the present case, the interval 7–16 November was almost geomagnetically quiet (except for a mild, extended storm during 11–15 November). Hence the average daily variation for these 10 (or less, as available) days was considered as a reasonable estimate of the background. (This does not ensure that the pattern would be representative of absolutely quiet conditions, but mild storm effects are not similar on successive days. Hence, averaging over several quiet and even some mildly disturbed days could be considered as a reasonably good background. This point will always remain subjective and debatable, but nothing much better can be done about it.) Then, two methods were employed. In one method, the background was subtracted from the actual hourly values. The deviations $f o$F2 minus $f o$F2 (average) were considered as anomalies (in MHz) and will be called henceforth as Anomalies, plotted in Fig. 1c. Positive deviations are painted black and negative deviations are shown as hatched. This location has some anomalies during 7–16 November, but the deviations are small as compared to those of other intervals. The storm effects are mostly positive, during 29–30 October and 20–21 November, but also during 4 November, when there was a small storm (D_{st} -89 nT). In the second method, the ratio of hourly $f o$F2 to $f o$F2 (average) was calculated. Henceforth, these will be called Ratios and are shown in Fig. 1d. The fluctuations (anomalies and ratios) in Figs. 1c and 1d are very similar, so any one of these can be used for the study. Small differences are mainly at low values of $f o$F2. Thus, a $f o$F2 value of, say, 8 MHz increasing to 9 MHz, would imply an anomaly of $+1$ MHz and a ratio of 1.125 (12.5% increase). However, a $f o$F2 of, say, 2 MHz increasing to 3 MHz, would also imply an anomaly of $+1$ MHz, but an enormously large ratio of 1.50 (50% increase).

The above procedure could be adopted only for data of 41 locations (out of 211) in which data were available at the website for Event X and/or Event Y, as listed in Table 1. Figures 2 and 3 show the plots, for Event X in the left half and Event Y in the right half. The top plots are for D_{st}. In Fig. 2, other plots are for $f o$F2 anomalies at (a) 10 stations (latitudes from Thule in the north to Port Stanley in the south) in longitudes near about $-65°$ (i.e. 65° W) and (b) another 10 stations (latitudes from Tromsø in the north to Grahamstown in the south) in longitudes near about 12° (i.e. 12° E). Similarly, in Fig. 3, plots are for $f o$F2 anomalies at (a) 18 stations (latitudes from Manzhouli in the north to Christchurch in south) in longitudes near about 135° (i.e. 135° E) and (b) for another 3 stations (College, King Salmon, Dyess, latitudes north) in longitudes near about 225° (i.e. 135° W). The following may be noted:

Event X (28–31 October 2003):

1. In Fig. 2a, left half, there is considerable latitudinal variation in the patterns, with roughly negative deviations in high latitudes and positive deviations in middle and low latitudes, but there are negative deviations at middle latitudes also. There is no systemetic movement of troughs from higher to lower latitudes as envisaged in the "average" pattern of the various models, indicating that localized electric fields rather than general global fields may be dominating and producing narrow troughs. Also, positive deviations seem to occur interspersed with negative deviations in an irregular way. Thus, ionospheric storm-time anomalies do not seem to have any reliable general pattern in individual storms. Patterns seem to vary largely from storm to storm. As such, predictions based on general patterns could be grossly inadequate and misleading for users like aviation pilots.

2. The most striking feature is the large positive deviations on 28 October, the day before the D_{st} storm commencement. Such pre-storm anomalies were pointed out earlier in Kane (1973 a,b; 1975), but do not seem to have received much attention by other workers, except by Danilov and Belik (1991, 1992). (These pre-storm positive anomalies are different from the F2-layer storm-like phenomena during geomagnetically quiet times observed by some Russian scientists in the 1980s.) If true, these could have very important implications, namely, these could be considered as precursors of geomagnetic disturbances. Such pre-storm increases can be seen in some of the plots in Araujo-Pradere and Fuller-Rowell (2002) also but have been ignored by them, and matching is discussed only starting from the main phase onwards.

3. Since all data reported to WDCs are in UT, we do not expect any error on the account of date and hour identification, unless the data have been reported for a wrong date (error of one date due to time zone differences).

4. In Fig. 3a, left half, too, large positive deviations are noticed throughout, from $\sim$24 h before the storm commencement (28 October) to well after the main phase recovery (31 October–1 November), but there is no systematic latitude dependence. Data for 29 October are

Table 1. Data used for the Halloween events X (29–31 October 2003) and Y (20–21 November 2003) and the giant event Z (13–14 March 1989).

	Station	code	Lat	Long	Lat	Long	Events	0–45	45–90	90–135	135–180	180–225	225–270	270–315	315–360
			Geographic		Geomagnetic			Longitude distribution East (in °)							
	Northern Hemisphere (NH) high latitudes (>50° N)														
1	Thule/Qanaq	THJ77	77.5° N	290.8° E	88.8° N	012.5° E	X, Y							*	*
2	Tromsø	TR169	69.7° N	019.0° E	67.0° N	117.5° E	X, Y	*							
3	Sondrestrom	SMJ67	67.0° N	310.0° E	77.1° N	035.8° E	X, Y							*	*
4	College	CO764	64.9° N	212.2° E	65.0° N	257.9° E	X, Y				*				
5	Yakutsk	YA462	62.0° N	129.6° E	51.2° N	194.8° E	Z			*					
6	Podkamennaya	TZ362	61.6° N	090.0° E	50.8° N	165.4° E	Z			*					
7	Narssarssuaq	NQJ61	61.2° N	314.6° E	70.9° N	038.5° E	X, Y							*	*
8	Leningrad	LD160	60.0° N	030.7° E	56.1° N	118.3° E	Z	*							
9	Uppsala	UP158	59.8° N	017.6° E	58.3° N	106.9° E	Z	*							
10	Churchill	CH958	58.8° N	265.8° E	68.7° N	324.9° E	Z						*		
11	King Salmon	KS759	58.7° N	203.4° E	57.9° N	257.2° E	X, Y				*				
12	South Uist	UI057	57.4° N	352.7° E	60.9° N	081.2° E	Z								
13	Sverdlovsk	SV256	56.4° N	058.6° E	48.5° N	139.6° E	Z			*					
14	Gorky	GK156	56.1° N	044.3° E	50.2° N	127.7° E	Z	*							
15	Moscow	MO155	55.5° N	037.3° E	50.4° N	123.2° E	Z	*							
16	Kaliningrad	KL154	54.7° N	020.6° E	53.0° N	106.4° E	Z	*							
17	Juliusruh/Rügen	JR055	54.6° N	013.4° E	54.3° N	099.7° E	X, Y, Z	*							
18	Novosibirsk	NS355	54.6° N	083.2° E	44.2° N	158.9° E	Z			*					
19	St Peter-Ording	PE054	54.0° N	009.3° E	37.2° N	088.1° E	Z	*							
20	Goosebay	GSJ53	53.3° N	299.2° E	64.4° N	014.0° E	X, Y							*	*
21	Petropavlovsk	PK553	53.0° N	158.7° E	44.9° N	219.9° E	Z				*				
22	Irkutsk	IR352	52.5° N	104.0° E	41.2° N	175.5° E	Z			*					
23	Fairford	FF051	51.7° N	358.2° E	54.3° N	082.8° E	X, Y								
24	Chilton	RL052	51.6° N	358.7° E	54.1° N	083.2° E	X, Y								
25	Slough	SL051	51.5° N	359.4° E	54.0° N	084.4° E	Z								
26	Kiev	KV151	50.5° N	030.5° E	47.1° N	113.3° E	Z	*							
27	Dourbes	DB049	50.1° N	004.6° E	51.7° N	088.9° E	Z	*							
	Northern Hemisphere (NH) middle latitudes (30° N–50° N)														
28	Karaganda	KR250	49.8° N	073.1° E	40.3° N	149.8° E	Z		*						
29	Manzhouli	ML449	49.6° N	117.5° E	38.4° N	186.5° E	X, Y			*					
30	Lannion	LN047	48.5° N	356.7° E	52.0° N	080.1° E	Z								
31	Khabarovsk	KB548	48.5° N	135.1° E	38.1° N	201.3° E	Z				*				
32	Argentia	AFJ49	47.3° N	306.0° E	58.9° N	021.6° E	Z							*	*
33	Bekescsaba	BH148	46.7° N	021.2° E	45.2° N	103.2° E	Z	*							
34	Poitiers	PT046	46.6° N	000.3° E	49.2° N	083.0° E	Z	*							
35	Novokazalinsk	NK246	45.5° N	062.1° E	37.6° N	139.6° E	Z		*						
36	Wakkanai	WK545	45.4° N	141.7° E	35.5° N	207.3° E	Z				*				
37	Sofia	SQ143	42.7° N	023.4° E	41.0° N	103.9° E	X, Y, Z	*							
38	Millstone Hill	MHJ45	42.6° N	288.5° E	53.9° N	358.7° E	X, Y							*	*
39	Rome	RO041	41.8° N	012.5° E	42.3° N	093.2° E	X, Y, Z	*							
40	Tashkent	TQ241	41.3° N	069.6° E	32.3° N	145.2° E	Z		*						
41	San Vito	VT139	40.6° N	017.8° E	41.1° N	098.5° E	X, Y	*							
42	Beijing	BP440	40.0° N	116.3° E	28.8° N	174.1° E	X, Y								
43	Boulder	BC840	40.0° N	254.7° E	48.9° N	318.7° E	Z						*		
44	Akita	AK539	39.7° N	140.1° E	29.8° N	206.8° E	Z				*				
45	Lisbon	LE038	38.7° N	350.7° E	43.3° N	070.4° E	Z								
46	Athens	AT138	38.0° N	023.6° E	36.4° N	102.5° E	X, Y	*							
47	Ashkhabad	AS237	37.9° N	058.3° E	30.4° N	134.5° E	Z		*						
48	Wallops Is	WP937	37.8° N	284.5° E	49.2° N	353.9° E	X,Y							*	*
49	Gibilmanna	GM037	37.6° N	014.0° E	37.8° N	093.2° E	Z	*							
50	Seoul (Osan Ab)	SU437	37.2° N	126.6° E	26.3° N	195.0° E	X, Y			*					
51	Kokubunji	TO535	35.7° N	139.5° E	25.7° N	206.7° E	Z				*				
52	Point Arguello	PA836	34.6° N	239.4° E	42.3° N	302.4° E	Z						*		
53	Dyess	DS932	32.4° N	260.3° E	42.0° N	326.7° E	X, Y						*		
54	Yamagawa	YG431	31.2° N	130.6° E	20.6° N	199.1° E	Z			*					
55	Eglin Afb	EG931	30.4° N	273.3° E	41.1° N	341.2° E	X, Y							*	*
	NH and SH low latitudes (30° N–30° S)														
56	Chongqing	9429	29.5° N	106.4° E	18.2° N	177.1° E	X, Y			*					
57	Okinawa	OK426	26.3° N	127.8° E	15.5° N	196.9° E	Z			*					
58	Chung-Li	CL424	24.9° N	121.2° E	13.8° N	190.9° E	Z			*					
59	Guangzhou	GU421	23.1° N	113.4° E	11.8° N	183.5° E	X, Y			*					
60	Maui	MA720	20.8° N	203.5° E	21.2° N	269.6° E	Z					*			
61	Puerto Rico	PRJ18	18.5° N	292.8° E	29.8° N	003.5° E	X, Y							*	*
62	Hainan	HA419	18.3° N	109.3° E	07.8° N	180.2° E	X, Y			*					
63	Dakar	DKA14	14.8° N	341.6° E	21.4° N	056.0° E	Z								
64	Manila	MN414	14.6° N	121.1° E	03.6° N	191.1° E	Z			*					
65	Ouagadougou	OU012	12.4° N	358.5° E	16.2° N	071.6° E	Z								
66	Vanimo	VA50L	02.7° S	141.3° E	12.3° S	212.5° E	X, Y, Z				*				

Table 1. Continued.

|	Station	code	Lat	Long	Lat	Long	Events								
			Geographic		Geomagnetic			0–45	45–90	90–135	135–180	180–225	225–270	270–315	315–360
67	Ascension	AS07R	07.9° S	012.4° E	06.6° S	082.0° E	X, Y	*							
68	Port Moresby	PY50R	09.4° S	147.1° E	18.3° S	219.2° E	X, Y				*				
69	Jicamarca	JI91J	12.0° S	283.2° E	00.7° N	353.7° E	X, Y							*	*
70	Darwin	DW41K	12.4° S	130.9° E	22.9° S	202.7° E	X, Y			*					
71	Tahiti	TT71P	17.7° S	210.7° E	15.2° S	284.4° E	Z					*			
72	Townsville	TV51R	19.3° S	146.7° E	28.5° S	220.4° E	X, Y, Z				*				
73	Learmonth	LM42B	21.9° S	114.0° E	33.0° S	185.3° E	X, Y			*					
74	Brisbane	BR52P	27.5° S	152.9° E	35.4° S	228.3° E	X, Y				*				
75	Norfolk Is	NI63_	29.0° S	168.0° E	34.5° S	244.6° E	X, Y				*				
	Southern Hemisphere (SH) middle latitudes (30° S–50° S)														
76	Mundaring	MU43K	32.0° S	116.2° E	43.2° S	187.7° E	X, Y, Z			*					
77	Grahamstown	GR13L	33.3° S	026.5° E	33.9° S	089.4° E	X, Y, Z	*							
78	Camden	CN53L	34.0° S	150.7° E	42.0° S	227.6° E	X, Y, Z				*				
79	Canberra	CB53O	35.3° S	149.0° E	43.7° S	225.7° E	X, Y, Z				*				
80	Hobart	HO54K	42.9° S	147.2° E	51.4° S	225.9° E	X, Y				*				
81	Christchurch	GH64L	43.6° S	172.8° E	47.7° S	253.5° E	X, Y				*				
	Southern Hemisphere (SH) high latitudes (>50° S)														
82	Port Stanley	PSJ5J	51.7° S	302.2° E	40.6° S	010.3° E	X, Y, Z							*	*
83	Argentine Is	AIJ6N	65.2° S	295.7° E	54.0° S	004.4° E	Z							*	*
	41 XY, 52 Z, total 93, but 10 common XYZ														
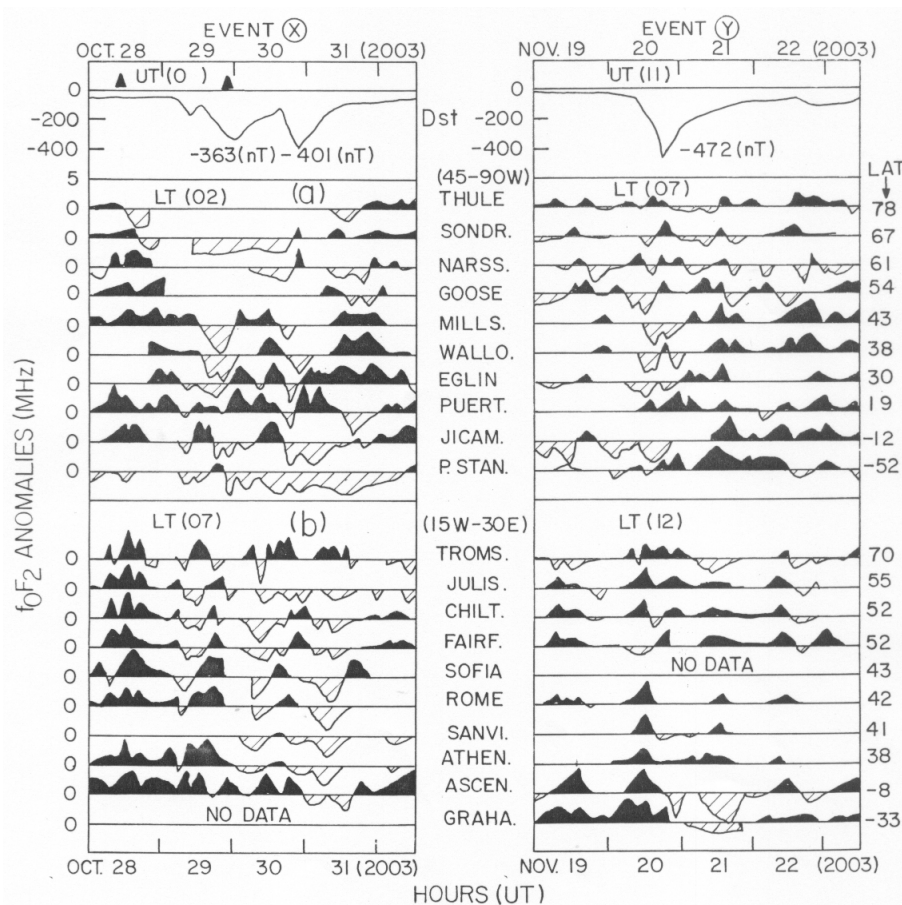
Fig. 2. Plots for Event X (28–31 October 2003) in the left half and Event Y (19–22 November 2003) in the right half, for D_{st} (top plots) and the $f o$F2 anomalies (MHz) for stations in different latitudes (north to south, indicated on the right) and longitude belts, **(a)** 45° W–90° W, **(b)** 15° W–30° E. Vertical lines mark the storm commencements. Positive deviations are painted black, negative deviations are shown as hatched.
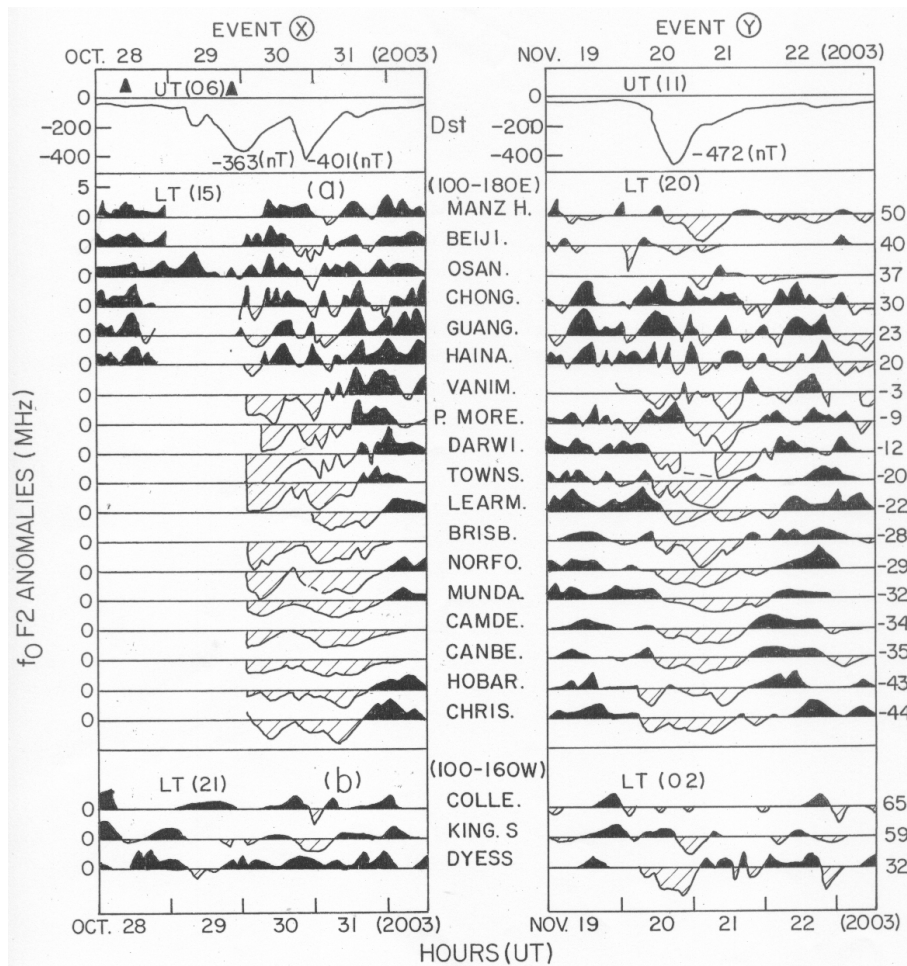
Fig. 3. Same as Fig. 2, for longitude belts **(a)** 100° E–180° E, **(b)** 100° W–160° W.

missing for many locations, particularly in Australia (which is a pity as their network generally has very good continuous data), and for 30 October onwards, severe negative effects are seen, probably because the end of October is almost summer for these locations.

5. In Fig. 3b, there are mainly positive deviations for all 3 locations in the Northern Hemisphere, before, during and after the main phase.

Event Y (19–22 November 2003):

1. In Fig. 2a,b, right half, the anomalies are mostly positive, though one would have expected strong negative effects at least for Port Stanley (52° S), where 20 November is almost summer. Instead, Jicamarca (12° S) in low latitude shows large negative deviations before and during the storm commencement, and positive effects thereafter. The reliability of the reported values is not known and spread F is very frequent at Jicamarca. Also, since 9–16 November was not completely quiet, the use of the average for these days as background might not be fully adequate. However, since the same background is used for subtraction for the X event as

well as the Y event, and the X event (Fig. 2a, left half, Jicamarca plot) does not show large negative deviations before the storm, the large negative deviations before and during the storm commencement in the Y event (Fig. 2a, right half, Jicamarca plot) could be genuine. However, since we have not examined the original data for spread effects, etc., a doubt will remain about this feature.

2. In Fig. 3a, right half, very strong negative effects are seen during the main phase in the Australian region as expected, but positive effects before the storm are embarrassing. In the north, effects are mostly positive.

3. In Fig. 3b, right half, for College and King Salmon, effects are small, but Dyess (32° N, 100° W) shows strong negative effects not expected for a northern midlatitude station in winter. A few hundred kilometers away, Eglin (30° N, 87° W) (Fig. 2b, right half) showed no such strong negative effects.

To bring out the latitude and longitude dependence more clearly and with more confidence, data for nearby locations were averaged. The plots are shown in Fig. 4, for Event X
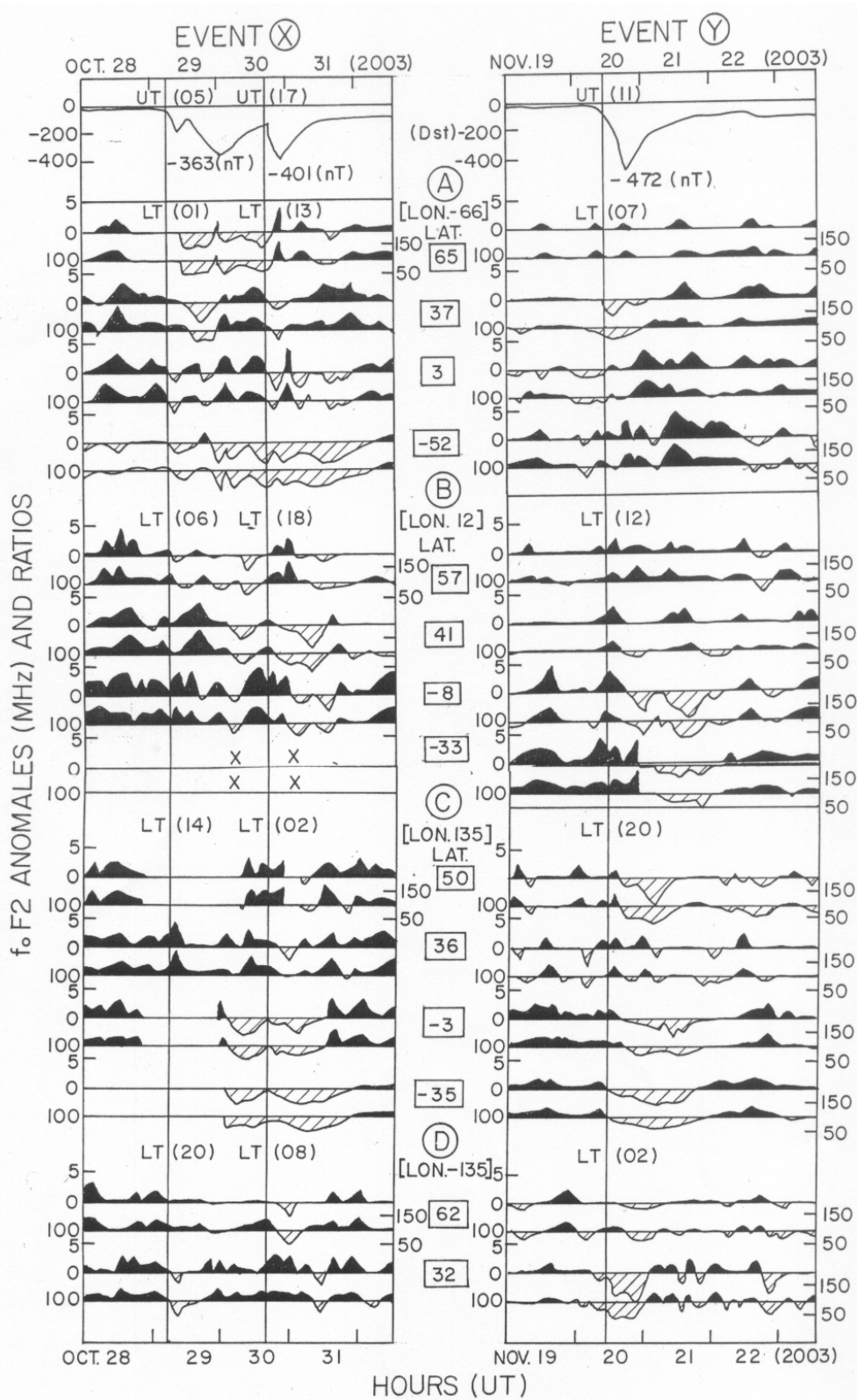
Fig. 4. Plots for Event X (28–31 October 2003) in the left half and Event Y (19–22 November 2003) in the right half, for D_{st} (top plots) and the $f o$F2 anomalies (MHz) and ratios (one below the other) for averages of stations in different average latitudes (north to south, indicated in the middle) and average longitudes **(A)** −66° i.e. 66° W, **(B)** +12° i.e. 12° E, **(C)** +135° i.e. 135° E and **(D)** −135° i.e. 135° W. Vertical lines mark the storm commencements. Positive deviations are painted black, negative deviations are shown as hatched.

in the left half and Event Y in the right half. For each latitude group, two plots are shown one below the other, namely anomalies (in MHz) and ratios (around 100), just to show that these two are almost alike. Four longitude zones are considered, namely around A ($-66°$ or $66°$ W), B ($12°$ or $12°$ E), C ($135°$ or $135°$ E) and D ($-135°$ or $135°$ W). The following may be noted:

Event X:

1. In Fig. 4, left half, the top plot is for D_{st}. The next four plots are for average latitudes $65°$ N, $37°$ N, $3°$ N and $52°$ S, for longitude group A around $66°$ W. The high latitudes ($>50°$) show negative effects as expected, in both hemispheres.

2. At northern middle latitudes ($37°$ N), effects are positive elsewhere but negative on the storm day (29 October). At low latitudes, effects are mostly positive. Positive effects are seen starting even before the storm commencement, and continuing into the storm. Such behavior is not envisaged in any storm model.

3. The next four plots are for average latitudes $57°$ N, $41°$ N, $8°$ S and $33°$ S, for longitude group B around $12°$ E. Here, effects are mostly positive on 29 October but negative on 30–31 October. Thus, a mixed effect is seen, probably because of the two separate storms of 29 October and 30 October, but strong positive effects are seen before the storm.

4. The next four plots are for average latitudes $50°$ N, $36°$ N, $3°$ S and $35°$ S, for longitude group C around $135°$ E. Here again, effects are mostly positive on 29 October (lots of data missing) but negative on 30–31 October, but strong positive effects are seen before the storm.

5. The next two plots are for average latitudes $62°$ N, $32°$ N, for longitude group D around $135°$ W. Here again, effects are mostly positive or slightly negative on 29 October, but strong positive effects are seen before the storm.

Event Y:

1. In Fig. 4, right half, the longitude group A has mostly positive effects at all latitudes, though the storm is during the morning hours. A strong negative effect was expected in southern high latitudes, because of local summer. Thus, the behavior is not consistent with any storm model.

2. For the longitude group B, the storm occurred at about noon, and effects were positive to start with (and even before the storm commencement) and negative in the evening and night hours.

3. For the longitude group C, the storm occurred in the evening, and effects were mostly negative.

4. For the longitude group D, the storm occurred at about midnight, and effects were small at high northern latitudes and negative for a northern midlatitude.

Thus, whereas some effects are as per model prediction, considerable disagreements or distortions (deviations not conforming with models) occurred in many instances. However, these distortions did not have any systematic dependence on latitudes or local times. On the whole, it looks like local electric field perturbations and composition changes are more dominant than the general patterns envisaged in models. In particular, positive deviations seem to occur more frequently than expected, particularly in the 24-hour pre-storm interval. A question that may arise is. How magnetically quiet is the pre-storm period? We have used here the D_{st} index and it shows sharp changes (depressions exceeding 350 nT) only on 29 October and 20 November. D_{st} values are available hourly and we consider these better than K_p values available every 3 h. On 28 October, the D_{st} depressions were less than 50 nT. However, some workers use K_p. In the present case, the K_p values were about 9 (highest possible value) on 29–30 October and 20 November, while values a few days earlier were 5 or less, considered only as weak or moderate. On 28 October, the 3-hourly K_p values were, 3, 5−, 4−, 5−, 3−, 4, 3+, 4. In principle, one can argue that the positive ionospheric anomalies on 28 October could be associated with the moderate geomagnetic disturbance of some K_p values of 5−, present even on 28 October, but we feel that just the two stray low 5− values of K_p could not have produced so strong ionospheric positive anomalies. This is, however, a subjective judgement, and in geophysics, strange things can and do occur, so all possibilities need to be considered. All that we can say is, the association of the strong positive ionospheric anomalies of 28 October with moderate K_p is possible but not probable.

Figure 5 shows two examples from the plots in Araujo-Pradere and Fuller-Rowell (2002), where their (empirical) model estimates were grossly different from the observations, both qualitatively and quantitatively. The interval shown is 5–9 April 2000 and the storm started at about 18:00 UT on 6 April (marked by vertical line). The expected (empirical) STORM model values (thick lines) show a negative storm, starting at the geomagnetic main phase and lasting for almost 48 h, with a minimum ratio of 0.6 (40% decrease) for Boulder (northern midlatitude) and 0.8 (20% decrease) for Port Stanley (southern high latitude). Actually, the observed values for Boulder showed a decrease (marked hatched) of ∼60% (instead of 40%) but for only for the first 12:00 UT hours of 7 April, and large positive effects for the rest of the time, including much before and much after the storm interval. Port Stanley showed large positive effects before and during the storm, and a negative effect (40%) only in the latter half of 7 April and small negative effects thereafter. We do not know for certain how the model prediction information is used by aeroplane pilots, but in the present case (storm of 6 April 2000), the model estimates (thick plot) would have certainly misled considerably the

pilots overflying Boulder or Port Stanley. The positive effects before the storm are quite large (30–40%) and the pilots would have been perplexed, as these do not appear, in the predictions. In their paper, Araujo-Pradere and Fuller-Rowell (2002) have presented 75 panels (for 15 stations for 5 storms in the year 2000, in their Figs. 4a–e, like those shown here in our Fig. 5). In all of these, their gray lines represent the outputs of their STORM model and these are mostly depressions (negative storms), starting at the geomagnetic storm commencement and intensifying in the next few tens of hours to as much as −30%. Only 10 (out of 75) show positive storms in the model values of southern midlatitudes, with increases of only about 10%. Thus, a negative storm seems to be a more certain feature, while positive storm effects seem to be small and uncertain. In their 75 panels (15 stations, 5 storms), more than half show substantial observed positive effects (∼20% increases above normal) before the storm commencement, but these have been ignored by those authors.

4 The giant event of 13 March 1989 (Event Z)

The D_{st} magnitude −589 nT of this event was the largest ever recorded since IGY, when the index D_{st} was formulated. The event had severe effects on the terrestrial environment (Allen et al. 1989). For this event, ionospheric effects have been reported in many publications (e.g. Batista et al., 1991; Greenspan et al., 1991; Huang and Chang, 1991; Lakshmi et al., 1991; Morton et al., 1991; Binachi et al., 1992; Rich and Denig, 1992; Yeh et al., 1992; Rasmussen and Greenspan, 1993; and probably many others). Many of these refer to a few stations in the equatorial and low latitudes in the American and Asian sectors and report large decreases or up and down oscillations. However, among these, Yeh et al. (1992) analyzed data from 52 ionosonde stations and 12 total electron content observing stations. Their global data showed a longitudinal dependence of the storm behavior, a worldwide depression of diurnal maximum foF2 (sometimes accompanied by a large rise in h'F2), TIDs, large-scale standing oscillations, hemispheric asymmetry, and suppression of equatorial anomaly. Thus, almost every ionospheric feature showed large deviations from normal ionospheric patterns. In the present communication, a similar analysis is presented, illustrated in a slightly different way, namely, anomalies. For this event, data were available on the website for only 52 locations (out of 211) and only 10 of these were common to those for the Halloween events. The plots for anomalies (MHz) only (not ratios) are shown in Fig. 6, not for individual locations but for avearges for nearby locations (the number of stations used for each plot is mentioned in circles). The whole period 8–17 March 1989 is plotted so that the effects of the minor storm of 8–9 March can be compared with those of the giant event of 13–14 March 1989 and with the quiet period in between. Anomalies (MHz) are plotted separately for the Northern Hemisphere (NH) high (>50° N) latitudes and middle (30° N–50° N) latitudes, NH and SH combined
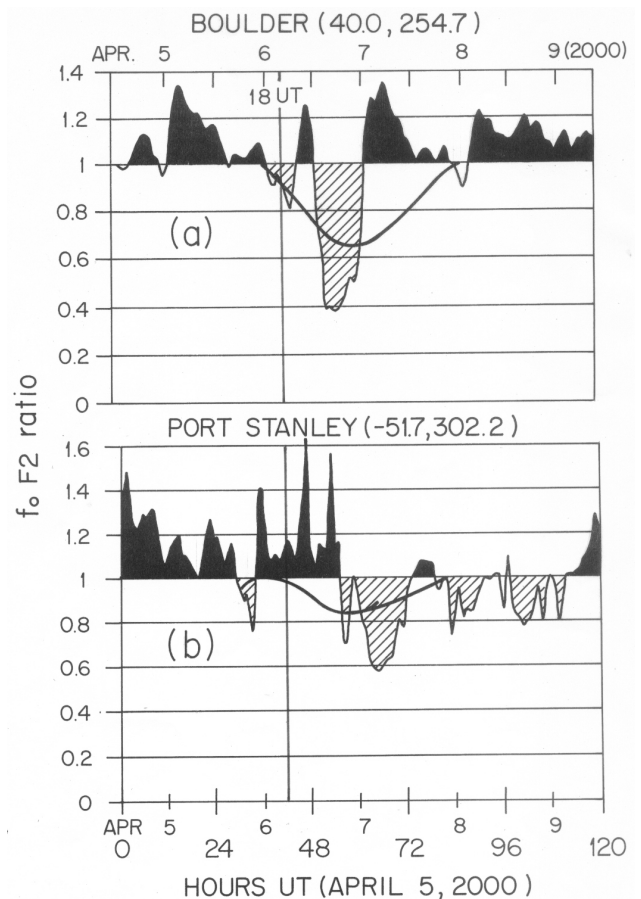

Fig. 5. Plots of foF2 ratios for the interval 5–9 April 2000 (storm occurred during 6–7 April) for Boulder and Port Stanley (read out from Araujo-Pradere and Fuller-Rowell, 2002). The thick line is their (empirical) STORM model prediction and full lines are observed values. Positive deviations are painted black, negative deviations are shown as hatched.

low latitudes (30° N–30° S) and for the Southern Hemisphere (SH) high (>50° S) latitudes and middle (30° S–50° S) latitudes. In each, successive plots are for progressive longitudes (A1, A2, B1, B2, C1, C2, D1, D2, each of 45° range), so that LT effects can be distinguished. The following may be noted:

1. The mild storm of 8–9 March seems to have substantial storm effects (1–4 MHz), mostly negative, with some positive effects interspersed. There is no clear latitude or longitude (LT) dependence.

2. The giant storm of 13–14 March seems to be predominantly a very strong negative storm which would gladden the hearts of the modelers. It started at the geomagnetic main phase (marked by a vertical line), was intense during the next ∼24 h, irrespective of latitude and longitude (LT), recouped to almost the zero level (or even slightly positive at some middle latitudes) and then had a second negative swing lasting for another ∼24 h. Later, some positive effects appeared but on 17 March, some negative effects are seen even though geomagnetic
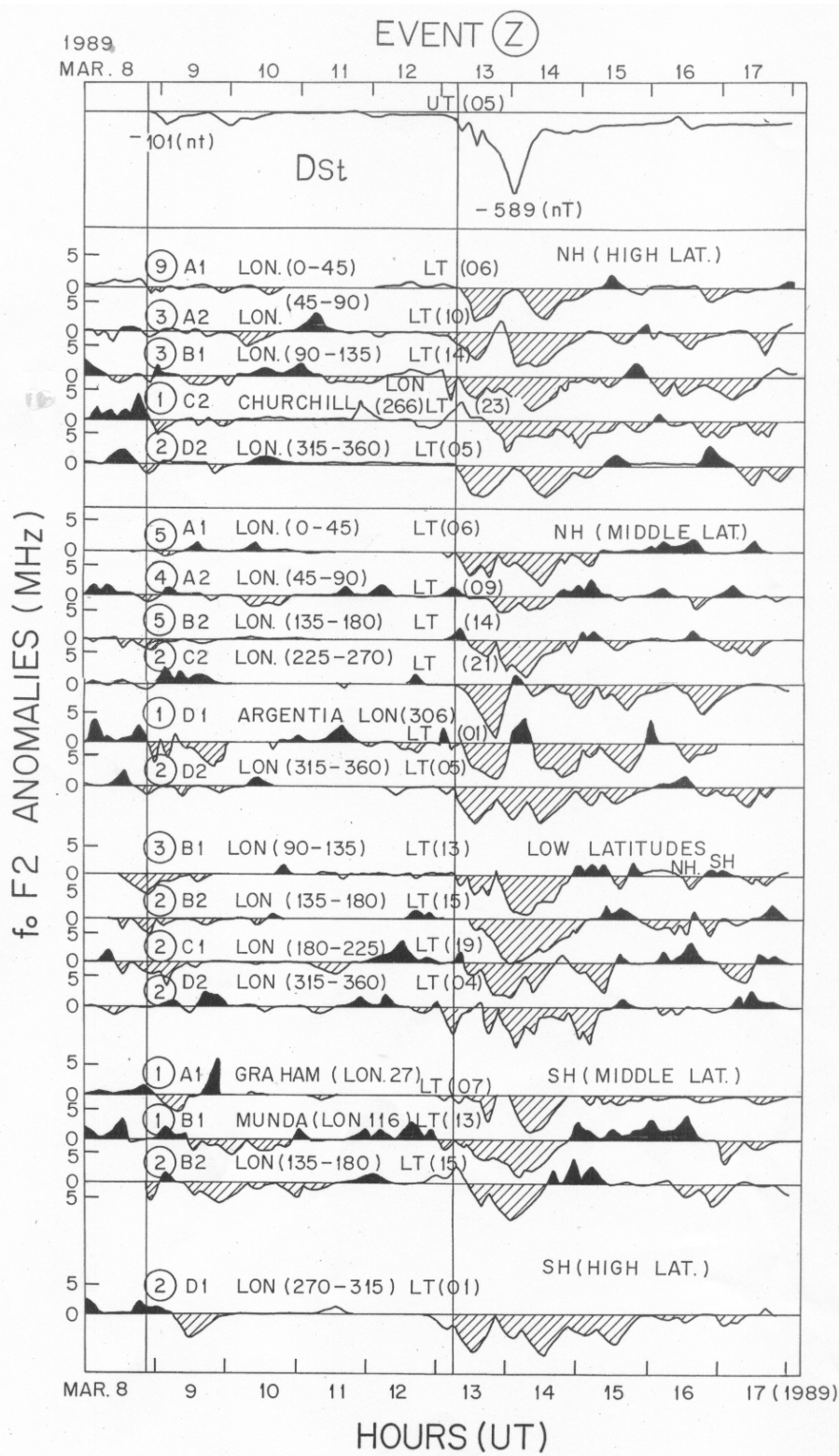
Fig. 6. Plots for the interval 8–17 March, 1989, containing the giant Event Z (13–14 March 1989) for D_{st} (top plot) and the $f o$F2 anomalies (MHz), for averages of stations in different latitudes: NH high latitudes (>50° N), NH middle latitudes (30° N–50° N), low latitudes (30° N–30° S), SH middle latitudes (30° S–50° S) and SH high latitudes (>50° S), for longitude ranges: A1 and A2, 0°–45° E, 45° E–90° E; B1 and B2, 90° E–135° E, 135° E–180° E; C1 and C2, 180° E–225° E, 225° E–270° E; D1 and D2, 270° E–315° E, 315° E–360° E. Numbers in circles indicate the number of stations involved in averaging. Vertical lines mark the storm commencements, for the minor storm of 8 March and the major storm of 13 March. Positive deviations are painted black, negative deviations are shown as hatched.

activity was quiet. Thus, storm effects lingered for 2–3 days before disappearing, and did not have any clear relation to LT.

3. Since this was an equinox period, no hemispherical differences were expected and none were observed. The negative storm started at the main phase commencement in both hemispheres, the maximum depressions of $f o$F2 were also comparable, but the evolution was not similar. Some locations showed two swings, some showed three, and others only one.

4. The positve effects were not seen near the storm commencement at any latitude or longitude and were seen at midlatitudes only after $\sim$24 h. In the case of this storm, no positive efects were seen at the main phase or before.

These results are roughly similar to those mentioned by Yeh et al. (1992), except for a few slightly different details. Also, altitude effects (hmF2) are not considered here, not because these are not important but because data were not available. This is a lacuna of this analysis. On the whole, this storm mostly conformed to the model expectations.

5 Conclusions and discussion

The global evolutions of $f o$F2 anomalies were examined for three very intense geomagnetic storms, namely the Halloween events of October–November 2003 (Event X, 29–30 October 2003, D_{st} −401 nT; Event Y, 20–21 November 2003, D_{st} −472 nT), and the largest D_{st} storm (Event Z, 13–14 March 1989, D_{st} −589 nT). Anomalies were estimated by subtracting quiet-day average daily (hour-to-hour) variation patterns from the observed hourly values. The following was noted:

1. For Event X (29–30 October, slight winter in NH and summer in SH), the troughs (negative storms) were clearly seen for $\sim$65° N at nighttime, but not at any other LTs. Troughs were strongly seen in high southern latitudes, as if this was a summer storm for SH (see also Pincheira et al., 2002). For northern midlatitudes as well as for low latitudes, there were very strong positive effects on 29 October, followed by negative effects the next day. The results for this storm are uncertain because firstly, it was a mixed, double storm (one on 29 October at 05:00 UT and another 36 h later on 30 October at 17:00 UT) and secondly, data for some locations were missing for 29 October.

2. For Event Y (20–21 November, winter in NH and summer in SH), there were no troughs in NH high latitudes for morning and evening hours but there were troughs for night. For midlatitudes and low latitudes, some longitudes showed strong negative effects in the early morning as expected, but some longitudes showed strong positive effects at noon and in the evening hours.

3. A striking feature was the presence of strong positive effects in the 24 h before the storm commencement, often continuing in the storm interval. This pre-storm feature was pointed out in earlier papers (Kane 1973 a, b; 1975) but does not seem to have attracted much attention. It is seen clearly, for example, in the plots of Araujo-Pradere and Fuller-Rowell (2002) (sample shown in our Fig. 5, where the positive effect is seen strongly before the storm and spilling into the storm interval). Such a feature appears only in the pre-storm 24 h but not earlier (for example, the positive deviations were not there on 27 October, but only on 28 October, one day before the storm day, 29 October 2003). If genuine, these would have a very important implication, namely a prediction potential with a 24-h precedence.

4. For Event Z (13–14 March 1989, equinox), all stations (all latitudes and longitudes) showed a very strong "negative storm" (and no positive storm at all) in the main phase. Also, the magnitudes (5–7 MHz) were consistently far greater than those for Event X or Y (hardly 5 MHz). True, the D_{st} for Event Z was large (−589 nT), but the D_{st} for Event Y was also large (−472 nT). Incidentally, the anomalies for a weak storm (8–9 March 1989) were also large (1–5 MHz). Thus, the magnitude of D_{st} does not seem to be exactly proportional to the anomaly magnitudes of $f o$F2. (This is understandable as D_{st} reflects the low latitude, high altitude currents at several Earth radii, while $f o$F2 changes are due to auroral high latitude ionospheric phenomena, with expansion towards low latitudes.) While all $f o$F2 depressions started at the storm commencement of Event Z, the further evolution was different at different longitudes (one swing, two swings, three swings) but not in any systematic way.

On the whole, whereas the March 1989 storm (Z event) conformed to the model expectations, the Halloween events of October–November 2003 showed ionospheric anomalies considerably different from the expected average patterns, and the differences seemed to be erratic, indicating strong local effects.

The positive deviations seen before the geomagnetic storm commencement are intriguing. Some explanations can be examined. Ionospheric parameters are known to have a high variability, even in quiet geomagnetic conditions. Forbes et al. (2000) estimated the Nmax variability for annual, semiannual and 11-yr solar cycle variations. Under quiet geomagnetic conditions, the standard deviations of Nmax variability were 25–35% at high frequencies (periods of a few hours to 1–2 days) and 15–20% at low frequencies (periods 2–30 days). This quiet-day ionospheric variability could be considered as random or could be due to "meteorological influences". Ionospheric variability increased with geomagnetic activity, increasing from low to high latitudes. This is the geomagnetic effect. Changes due to variations in solar photon flux are reported to be rather small by these authors.

However, Mendillo et al. (1974) showed for the Total Electron Content (TEC) measured at 20 locations during the great solar flare of 7 August 1972 that there were 15 to 30% TEC increases with a rise time of about 10 min, with larger increases at lower latitudes. This is the solar flare effect. Such effects can last several hours (but less than ~6) due to the slow recombination rate of the F region plasma. Recently, Tsurutani et al. (2005) examined the global ionospheric effects (TEC enhancements) of the 28 October 2003 solar flare and found 30% increases within a few minutes, lasting for ~3 h. Thus, some of the pre-storm positive changes (increases in $f o$F2) in the 24 pre-storm hours could be due to lingering effects of the additional ionization caused by strong solar flare effects. Rishbeth and Mendillo (2001) gave estimates of ionospheric variability as 20% by day and 33% by night. They found that a large part of F2-layer variability was linked to that of geomagnetic activity, and the rest to "meteorological" sources at lower levels of the atmosphere. As such, the positive effects before the geomagnetic storm commencement could be partly of meteorological origin. However, strong positive effects a few tens of hours before the beginning of the geomagnetic disturbances could not all be meteorological effects or natural quiet time day-to-day variability. Recently, Danilov (2001) has discussed this problem of positive phases which are sometimes observed several hours before the beginning of a magnetic disturbance (e.g. during 13–14 September 1973, observed by Danilov and Belik, 1991, 1992). The ionospheric positive storm during magnetic disturbances is attributed to the F2 layer uplifting due to vertical drift, plasma fluxes from the plasmasphere, and downwelling of the gas as a result of the storm-induced thermospheric circulation (Danilov and Belik, 1992; Prölss, 1995). But for positive phases occurring sometimes before the beginning of the magnetic storm, this scheme does not work, as there is still neither the depleted [O]/[N$_2$] nor storm-induced circulation. So, some other channel of penetration of the disturbed solar wind energy to ionospheric heights, other than the usual one which leads to the Joule heating and auroral precipitation, is needed. It could be the effect of soft particle precipitation (emanating from solar flares but reaching the Earth a few hours later) in the region of the dayside cusp, as the cusp is the only formation which starts to react to the coming geomagnetic disturbances before any geomagnetic index does: the cusp begins to move equatorward a few hours before the beginning of the D_{st} depletion (Danilov and Belik, 1992). However, no quantitative evaluation has been done so far and the role of electric fields, particularly its B_y component, needs to be considered. Danilov (2001) concludes that for F2 region responses to geomagnetic disturbances, there are still unsolved problems, the most acute ones being: appearance of positive phases before the beginning of the magnetic storms, the occurrence of strong negative phases at the equator, the role of vibrationally excited nitrogen in the forming of the negative phase, and the relation of positive phases to the dayside cusp. Further investigations are needed to resolve these problems.

References

Allen, J., Sauer, H., Frank, L., and Reiff, P.: Effects of the March 1989 solar activity, EOS Trans. AGU, 70, 1479, 1989.

Araujo-Pradere, E. A. and Fuller-Rowell, T. J.: STORM: An empirical storm-time ionospheric correction model, 2. Validation, Radio Sci. 37, 5, 1071, doi:10.1029/2002RS002620, 2002.

Batista, I. S., de Paula, E. R., Abdu, M. A., Trivedi, N. B., and Greenspan, M. E.: Ionospheric effects of the March 1989 magnetic storm at low and equatorial latitudes, J. Geophys. Res. 96, 13 943–13 952, 1991.

Binachi, C., Santis, A. D., Meloni, A., and Zolesi, B.: Magnetic and ionospheric effects of the strong magnetospheric storm of March 13th 1989 over Italy, Il Nuovo Cimento, 15, 1, 1992.

Buonsanto, M. J.: Ionospheric storms – A review, Space Science Reviews, 88, 563–601, 1999.

Danilov, A. D.: F-2 region response to geomagnetic disturbances, J. Atmos. Solar-Terres. Phys., 63, 441–449, 2001.

Danilov, A. D. and Belik, L. D.: Thermosphere-ionosphere interaction in a period of ionospheric storms, Geomagnetism and Aeronomy, 31, 2 157–167, 1991.

Danilov, A. D. and Belik, L. D.: Thermospheric composition and the positive phase of an ionospheric storm, Advan. Space Res., 12 10, 257–260, 1992.

Fejer, B. G.: The Electrodynamics of the Low-latitude Ionosphere: Recent Results and Future Challenges, J. Atmos. Solar Terr. Phys., 59, 1465–1482, 1997.

Forbes, J. M., Palo, S. E., and Zhang, X.: Variability of the ionosphere, J. Atmos. Solar-Terr., Phys., 62, 685–693, 2000.

Greenspan, M. E., Rasmussen, C. E., Burke, W. J., and Abdu, M. A.: Equatorial density depletions observed at 840 km during the great magnetic storm of March 1989, J. Geophys. Res., 96, 13 931–13 942, 1991.

Huang, Y. N. and Chang, K.: Ionospheric disturbances at the equatorial anomaly crest region during the March 1989 magnetic storm, J. Geophys. Res., 96, 13 953–13 965, 1991.

Kane, R. P.: Storm-time variations of F2, Annales de Geophysique, 29, 25–42, 1973a.

Kane, R. P.: Global evolution of F2-region storms, J. Atmos. Terr. Phys., 35, 1953–1966, 1973b.

Kane, R. P.: Global evolution of the ionospheric electron content during some geomagnetic storms, J. Atmos. Terr. Phys., 37, 601–611, 1975.

Lakshmi, D. R., Rao, B. C. N., Jain, A. R., Goel, M. K., and Reddy, B. M.: Response of the equatorial and low latitude F-region to the great magnetic storm of 13 March 1989, Ann. Geophys., 9, 286–290, 1991.

Mendillo, M., Klobuchar, J. A., and Fritz, R. B., et al.: Behavior of the ionospheric F region during the great solar flare of 7 August 1972, J. Geophys. Res., 79, 665–672, 1974.

Morton, Y. T., Mathews, J. D., and Zhou, Q.: Electron Concentration Configurations During the 13–14 March 1989 Geomagnetic Storm as Measured by Arecibo Incoherent Scatter Radar, Spring American Geophysical Union Meeting, Baltimore, MD, (28 May–1 June 1991), 1991.

Pincheira, X. T., Abdu, M. A., Batista, I. S., and Richards, P. G.: An investigation of ionospheric responses, and disturbance thermospheric winds, during magnetic storms over South American sector, J. Geophys. Res., 107(A11), 1379, doi:10.1029/2001JA000263, 2002.

Prölss, G. W.: Ionospheric F-region storms, in: Handbook of Atmospheric Electrodynamics, 2, edited by: Volland, H., CRC Press, Boca Raton, 195–248, 1995.

Prölss, G. W.: Magnetic Storm Associated Perturbations of the Upper Atmosphere, in: Magnetic Storms, (Eds.) Tsurutani, B. T., Gonzales, W. D., Kamide, Y., and Arballo, J. K., Geophysical Monograph 98, AGU, Washington, D. C., 1997.

Rasmussen, C. E. and Greenspan, M. E.: Plasma transport in the equatorial ionosphere during the great magnetic storm of March, 1989, J. Geophys. Res., 98, 285–292, 1993.

Rich, F. J. and Denig, W. F.: The major magnetic storm of 13–14 March 1989 and associated ionospheric effects, Can. J. Phys., 70, 510–525, 1992.

Rishbeth, H. and Mendillo, M.: Patterns of F2-layer variability, J. Atmos. Solar-Terr., Phys., 63, 1661–1680, 2001.

Szuszczewicz, E. P., Lester, M., Wilkinson, P., Blanchard, P., Abdu, M., Hanbaba, R., Igarashi, K., Pulinets, S., and Reddy, B. M.: A Comparative Study of Global Ionospheric Responses to Intense Magnetic Storm Conditions', J. Geophys. Res., 103, 11 665–11 684, 1998.

Tsurutani, B. T., Judge, D. L., and Guarnieri, F. L., et al.: The 28 October 2003 extreme EUV solar flare and resultant extreme ionospheric effects: Comparison to other Halloween events and the Bastille Day event, Geophys. Res. Lett., 32, L03S09, doi:10.1029/2004GL021475, 2005.

Yeh, K. C., Lin, K. H., and Conkright, R. O.: The global behavior of the March 1989 ionospheric storm, Canad. J. Phys., 70, 532–543, 1992.